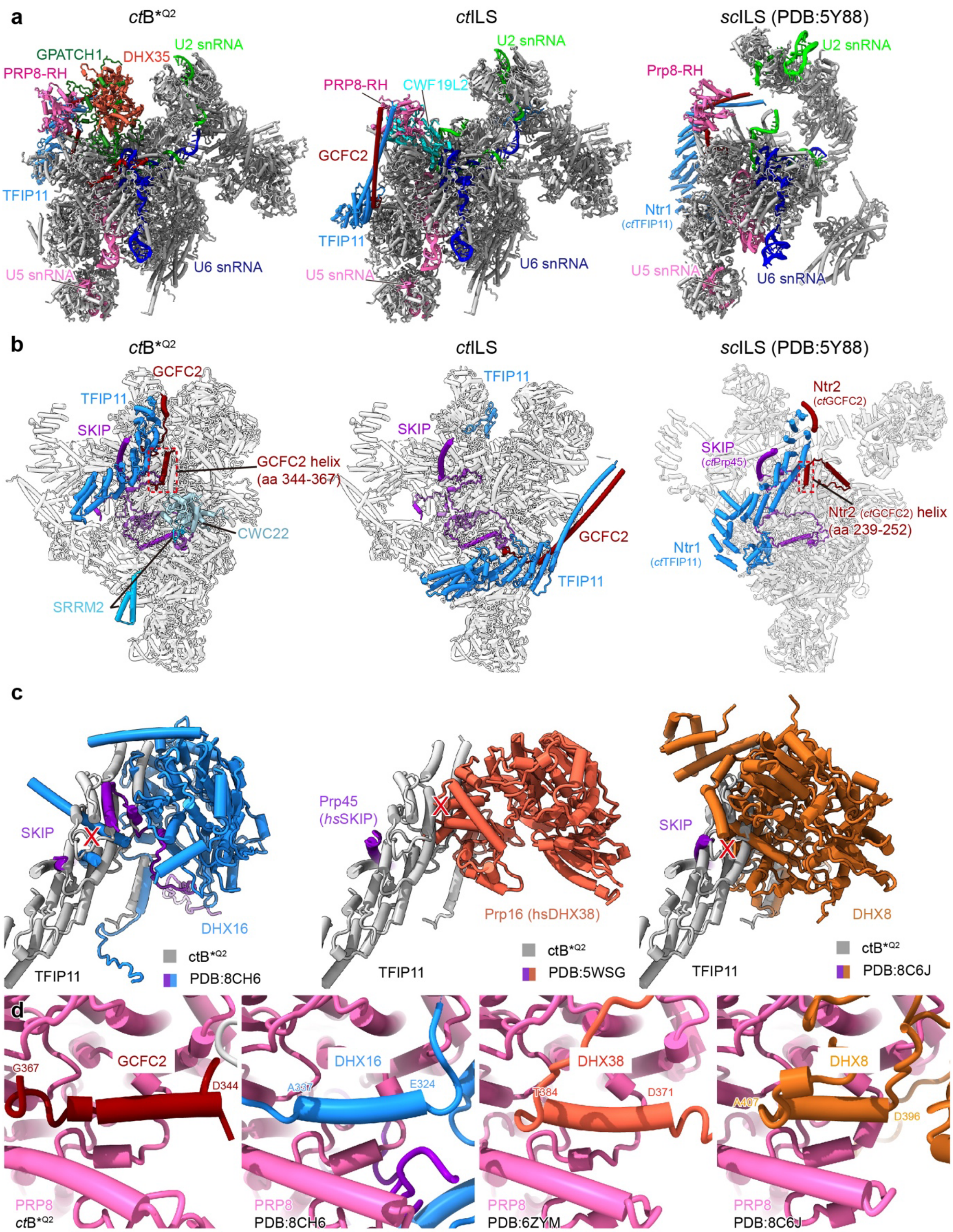

Figure S10: Structural comparison of the *ct*B*^{Q2}, *ct*ILS and *sc*ILS complexes.

a, Differences between *ct*B*^{Q2} (left), *ct*ILS (middle) and *sc*ILS (right) are highlighted: PRP8-RH domain (hot pink), GPATCH1 (green), DHX35 (tomato red), and CWF19 (green). **b**, Comparison of the position of the TFIP11-GCFC2 dimer in the *ct*B*^{Q2} (left), *ct*ILS (middle) and *sc*ILS (right) complexes. SRRM2 and CWC22 are present in *ct*B*^{Q2}

(left) but missing in *ct*ILS (right). Notably, TFIP11 binds to a similar region in *ct*B^{*Q2} as it does in baker's yeast *sc*ILS state. **c**, Overlay of TFIP11 from *ct*B^{*Q2} with the position of DHX16 (left, PDB: 8CH6), DHX38 (middle, PDB: 5WSG) and DHX8 (right, PDB: 8C6J) during B^{act} and C* complexes. **d**, Close-up view of the steric clash between GCFC2 (left, aa 344-367) and the binding sites for DHX16 (aa 324-337, PDB: 8CH6), DHX38 (aa 371-384, PDB: 6ZYM) and DHX8 (aa 396-407, PDB: 8C6J).